IOPscience iopscience.iop.org

Home Search Collections Journals About Contact us My IOPscience

Electrical current induced pinhole formation and insulator–metal transition in tunnel junctions

This article has been downloaded from IOPscience. Please scroll down to see the full text article.

2007 J. Phys.: Condens. Matter 19 176207

(http://iopscience.iop.org/0953-8984/19/17/176207)

View the table of contents for this issue, or go to the journal homepage for more

Download details:
IP Address: 129.252.86.83
The article was downloaded on 28/05/2010 at 17:53

Please note that terms and conditions apply.

IOP PUBLISHING JOURNAL OF PHYSICS: CONDENSED MATTER

J. Phys.: Condens. Matter **19** (2007) 176207 (9pp) doi:10.1088/0953-8984/19/17/176207

Electrical current induced pinhole formation and insulator–metal transition in tunnel junctions

J Ventura[1,2], **Z Zhang**[3,4], **Y Liu**[3,5], **J B Sousa**[1,2] **and P P Freitas**[1,3]

[1] IN, Rua Alves Redol, 9-1, 1000-029 Lisbon, Portugal
[2] IFIMUP, Rua do Campo Alegre, 678, 4169-007, Porto, Portugal
[3] INESC-MN, Rua Alves Redol, 9-1, 1000-029 Lisbon, Portugal
[4] Department of Optical Science and Engineering, Fudan University, Shanghai, People's Republic of China
[5] Department of Physics, Tongji University, Shanghai, People's Republic of China

E-mail: joventur@fc.up.pt

Received 22 February 2007
Published 28 March 2007
Online at stacks.iop.org/JPhysCM/19/176207

Abstract

Current induced resistance switching (CIS) was recently observed in thin tunnel junctions (TJs) with ferromagnetic (FM) electrodes and was attributed to electromigration of metallic atoms in nanoconstrictions in the insulating barrier. Here the CIS effect is studied in TJs with two thin (20 Å) non-magnetic (NM) Ta electrodes inserted above and below the insulating barrier. We observe resistance (R) switching for positive applied electrical current (flowing from the bottom to the top lead), characterized by a continuous decrease in resistance and associated with current-driven displacement of metallic ions from the bottom electrode into the barrier (thin barrier state). For negative currents, displaced ions return to their initial positions in the electrode and the electrical resistance gradually increases (thick barrier state). We measured the temperature (T) dependence of the electrical resistance of both thin- and thick-barrier states (R_b and R_B, respectively). Experiments showed a weaker $R(T)$ variation when the tunnel junction is in the R_b state, associated with a smaller tunnel contribution. By applying large enough electrical currents we induced large irreversible R decreases in the studied TJs, associated with barrier degradation. We then monitored the evolution of the $R(T)$ dependence for different stages of barrier degradation. In particular, we observed a smooth transition from tunnel- to metallic-dominated transport. The initial degradation stages are related to irreversible decreases in barrier thickness (without the formation of pinholes). Only for later stages of barrier degradation do we have the appearance of metallic paths between the two electrodes that, however, do not lead to metallic-dominated transport for small enough pinhole radius.

(Some figures in this article are in colour only in the electronic version)

© 2007 IOP Publishing Ltd Printed in the UK

1. Introduction

Tunnel junctions (TJs) are magnetic nanostructures consisting of two ferromagnetic (FM) layers separated by an insulator (I) [1]. The magnetization of one of the FM layers (pinned layer) is fixed by an underlying antiferromagnetic (AFM) layer. The magnetization of the other FM layer (free layer) reverses almost freely when a small magnetic field is applied. Due to spin dependent tunnelling [2] one obtains two distinct resistance (R) states corresponding to parallel (low R) or antiparallel (high R) pinned/free layer magnetizations. Large tunnel magnetoresistive ratios of over 70% in Al_2O_3-based [3] and 150% in MgO-based [4, 5] (currently reaching more than 400% [6]) tunnel junctions can be obtained, making them the most promising candidates for high performance, low cost, non-volatile magnetoresistive random access memories (MRAMs) [7]. Current research is focused on replacing magnetic field-driven magnetization reversal by a current induced magnetization switching (CIMS) mechanism [8, 9]. Such a goal was recently achieved in magnetic TJs [10, 11] for current densities $j \sim 10^7$ A cm^{-2}. On the other hand, Liu *et al* [12] observed reversible R changes induced by lower current densities ($j \sim 10^6$ A cm^{-2}) in thin FM/I/FM TJs. These changes were found to be of non-magnetic origin [13] and were attributed to electrical field-induced electromigration (EM) in nanoconstrictions in the insulating barrier [14–16]. This new effect, called current induced switching (CIS), can limit the implementation of the CIMS mechanism in actual MRAMs, and its understanding is then crucial for device reliability.

The influence of current induced switching on the behaviour of the transport properties of AFM/FM/NM/I/NM/FM tunnel junctions is studied here in detail (NM $\equiv$ non-magnetic). Resistance switching under relatively low positive electrical currents ($I \approx 20$ mA) produces a low resistance state due to local displacements of metallic ions from the bottom electrode into the barrier (thin barrier state). Applying sufficiently negative currents leads to the return of the displaced metallic ions from the barrier back into the electrode and so to an increase of the electrical resistance of the TJ (thick barrier state), virtually displaying a reversible behaviour. No time dependent phenomena were observed after each switching event [17], indicating that migrated Ta ions remain in deep energy minima inside the barrier. We compared the temperature (T) dependence between 20 and 300 K of the electrical resistance of the above thin- and thick-barrier states of the junction obtained after each switching (R_b and R_B, respectively), observing a smaller $R(T)$ variation in the thin-barrier R_b state.

Applying large currents ($|I| \gtrsim 80$ mA) leads to irreversible decreases in resistance due to enhanced barrier degradation. Successive switching under large $|I|$ produced a gradual evolution from tunnel- to metallic-dominated transport due to current-induced barrier weakening. This effect initially starts with an irreversible decrease in mean barrier thickness, followed by the establishment of metallic paths between the two electrodes. However, for small enough pinhole radius, tunnels still dominate transport ($\mathrm{d}R/\mathrm{d}T < 0$) and only subsequent current-induced growth of pinhole size leads to a metallic-like temperature dependence ($\mathrm{d}R/\mathrm{d}T > 0$).

2. Experimental details

We studied a series of ion beam deposited tunnel junctions, with thin *non-magnetic* Ta layers inserted just below and above the insulating AlO_x barrier. The corresponding complete structure was glass/bottom lead/Ta (90 Å)/NiFe (50 Å)/MnIr (90 Å)/CoFe (40 Å)/Ta (20 Å)/AlO_x (3 Å + 4 Å)/Ta(20 Å)/CoFe (30 Å)/NiFe (40 Å)/Ta (30 Å)/TiW(N) (150 Å)/top lead. Details on sample deposition and patterning processes were given previously in [15]. Notice that the studied TJ structure is similar to that of magnetic tunnel junctions grown for actual applications with the exception of the additional thin Ta layers, thus making comparisons

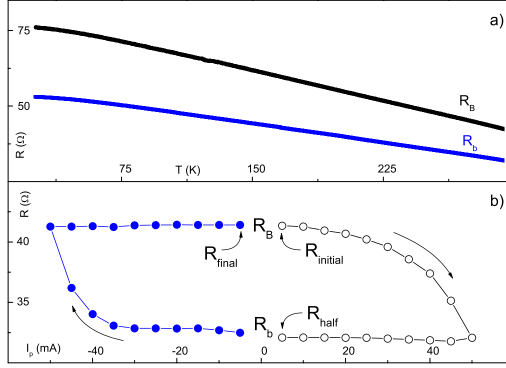

Figure 1. (a) Temperature dependence of the electrical resistance in the low (R_b; thin barrier) and high (R_B; thick barrier) CIS states of TJ1. (b) A half CIS cycle performed with $I_{max} = 50$ mA (open circles) that enabled us to change from the (initial) thick to the thin barrier state; the subsequent half CIS cycle recovers the thick barrier state (full circles) and displays a reversible behaviour.

with the FM/I/FM system easier. In particular, one can separate interface electric effects related to the particular metal layers bounding the oxide layer from the spin polarization effects originated from the FM layers. Electrical resistance and current induced switching were measured with a standard four-point dc method. Temperature dependent measurements were performed (on cooling) in a closed cycle cryostat down to 20 K [18, 19]. CIS cycles were obtained using the pulsed current method [13], providing the *remnant* resistance value of the TJ after each current pulse. We briefly describe some of the procedures used to measure CIS cycles [15]. Current pulses (I_p) of 1 s duration were applied to the junction, starting with increasing pulses from $I_p = 0$ (where we define the resistance as $R_{initial}$) up to a maximum $+I_{max}$, in small ΔI_p steps. The current pulses were then decreased through zero (half cycle, $R \equiv R_{half}$) down to negative $-I_{max}$, and then again to zero (R_{final}), to close the CIS hysteretic cycle. To discard non-linear $I(V)$ contributions, the junction remnant resistance was measured between current pulses, always using a low current of 0.1 mA, providing a $R(I_p)$ curve for each cycle. Positive current is here defined as flowing from the bottom to the top NM electrode. With the above definitions, one defines the CIS coefficient:

$$\mathrm{CIS} = \frac{R_{initial} - R_{half}}{(R_{initial} + R_{half})/2}, \tag{1}$$

and the resistance shift (δ) in each cycle:

$$\delta = \frac{R_{final} - R_{initial}}{(R_{initial} + R_{final})/2}. \tag{2}$$

3. Experimental results

A FM/NM/I/NM/FM tunnel junction with $R \approx 43\ \Omega$ and $R \times A \approx 170\ \Omega\ \mu\mathrm{m}^2$ (TJ1) was used to study current induced switching. A CIS cycle spanning pulse currents up to $I_{max} = 50$ mA is displayed in figure 1(b), giving CIS $= 25\%$ and $\delta = -0.1\%$ at room temperature. With increasing (positive) applied current pulse, switching starts at $I_p \gtrsim 20$ mA through a progressive (but increasingly pronounced) decrease in R until $I_{max} = 50$ mA. This switching is associated with local electrical current-driven displacement of Ta ions from the bottom electrode into the insulator [15], decreasing the effective barrier thickness and so the junction

resistance (thin barrier state; R_b). Even a small weakening of the barrier considerably lowers the tunnel resistance due to its exponential dependence on barrier thickness. Furthermore, the switching is asymmetric with respect to the applied current direction, as observed in previous studies [16, 15] (only ions from the bottom interface participate in electromigration). This effect was related to the particular sequence of the deposition and oxidation processes during fabrication of the TJ [16, 15].

The net atomic flux resulting from an applied electrical field is usually called electromigration. The electromigration force can be divided into two components: one acts in the direction of the electron flow (wind force) due to the transfer of momentum from electrons to the migrating ions; the other acts in the direction of the electrical field (direct force) and is due to the electrostatic interaction between the electrical field and the direct valence of the ion [20]. Usually, the wind force is much larger than the direct force. However, in our system, the ultra-thin barrier favours intense electrical fields, thus enhancing field-directed diffusion (direct force dominance). Additionally, high applied electrical currents produce large heating and thus thermally enhanced electromigration [15]. Our results indicate that such diffusion in our samples is essentially of a local character, ultimately causing pinhole formation (see below).

Returning to figure 1(b), the decrease of I_p from $+I_{max}$ to zero hardly affects the low resistance state. This indicates that displaced Ta ions remain trapped in deep local energy minima inside the barrier. Such a low R state then persists for current pulses down to -35 mA. However, when $I_p < -35$ mA the (reversed sign) driving force gets strong enough to initiate the return of the displaced ions into their initial positions in the NM layer (causing an increase in R), an effect which is rapidly enhanced until $I_p = -I_{max}$. We then have a thick barrier state (R_B), i.e. completely recovering the previous (negative) R-switching which occurred near $+I_{max}$. The subsequent change of I_p from $-I_{max}$ to zero, again leaves R essentially unchanged.

We then measured the temperature dependence of the electrical resistance of the TJ in its *thick* (R_B) and *thin* (R_b) barrier states (figure 1(a)). The resistance of the R_B state steadily increases with decreasing T from $R_B = 43\ \Omega$ at 300 K to 76 Ω at $T = 20$ K (figure 1(a)). Defining the relative change in R between 300 and 20 K as:

$$\alpha = \frac{R_{300\ K} - R_{20\ K}}{R_{300\ K}}, \tag{3}$$

so that $\alpha < 0$ (>0) indicates tunnel-dominated (metallic) transport, we obtain $\alpha_B = -78\%$ for the thick barrier state. On the other hand, after performing a positive half CIS cycle ($0 \to I_{max} \to 0$) at room temperature (figure 1(b); open circles), the tunnel junction was left in its thin barrier state, following the $R_b(T)$ measurements. The results now reveal a smaller increase in R from 300 K down to 20 K ($R_b \approx 32$ and 53 Ω, respectively) than in the $R_B(T)$ case, giving $\alpha_b = -66\%$, and so $\alpha_B < \alpha_b < 0$.

The $R_B(T)$ and $R_b(T)$ curves were fitted to the expressions for two- and three-step hopping [21] and phonon-assisted tunnelling [22], revealing a decrease of the hopping contributions and a slight increase of the phonon-assisted tunnelling when one goes from R_B to the R_b state. This is here attributed to the decrease of the barrier thickness (reducing the hopping contribution) and to enhanced excitation of phonons at the electrode/oxide interface by tunnelling electrons.

We also studied the effect of increasing barrier degradation on the (subsequent) temperature dependence of the electrical resistance of a tunnel junction. For this we performed CIS cycles with high I_{max} (in the 80–110 mA range), each successive one showing a large negative δ-shift at room temperature ($R_{final} \ll R_{initial}$), indicating a progressive and irreversible barrier weakening [15]. After each nth room temperature CIS cycle, we always measured $R(T)$ from 300 to 20 K. No temperature hysteresis was observed, so that on heating back

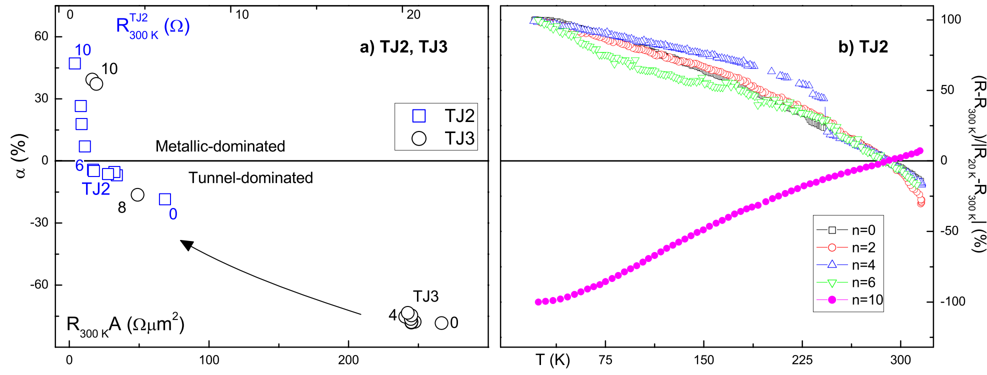

Figure 2. (a) The relative resistance change from 300 to 20 K (α) as a function of the $R \times A$ product (lower scale; for TJ2 and TJ3) and $R_{300\ \mathrm{K}}$ (upper scale; TJ3 only). A resistance decrease was induced by current-driven barrier degradation under high applied current pulses. The numbers in the figure indicate how many CIS cycles were performed before the corresponding α-data point was obtained. (b) Selected normalized $R(T)$ curves in the 300–20 K range (TJ2).

to room temperature, the nth value of the TJ resistance is essentially recovered. On the other hand, with increasing (n) cycling, the junction transport changed smoothly from tunnel-dominated ($\mathrm{d}R/\mathrm{d}T < 0$) to metallic-dominated ($\mathrm{d}R/\mathrm{d}T > 0$; figure 2(a)). Two tunnel junctions were used in this particular study: TJ2 with initial $R = 11.3\ \Omega$ ($R \times A = 67.8\ \Omega\ \mu\mathrm{m}^2$) and TJ3 with $R = 21.6\ \Omega$ ($R \times A = 259.2\ \Omega\ \mu\mathrm{m}^2$).

Both TJs initially ($n = 0$; before any CIS cycle) exhibit a tunnel-dominated $R(T)$ behaviour with $\alpha = -20\%$ and -75%, for samples TJ2 and TJ3, respectively (notice the smaller $R \times A$ product of TJ2). Subsequent CIS cycles with large I_{max} led to irreversible decreases of the resistance of the TJs and to a steady increase of α in both samples (figure 2(a)). Nevertheless, our $R(T)$ data still showed tunnel-dominated transport ($\alpha < 0$) down to $R \times A \approx 20\ \Omega\ \mu\mathrm{m}^2$. The last $R(T)$ measurement with tunnel-dominated behaviour displayed $\alpha = -3\%$ for TJ2 ($n = 6$; $R \approx 2.5\ \Omega$) and $\alpha = -15\%$ for TJ3 ($n = 8$; $R \approx 5\ \Omega$). Finally, further cycling ultimately leads to metallic behaviour, with, for example, $\alpha = 47\%$ for TJ2 ($n = 10$; $R = 0.65\ \Omega$) and $\alpha = 40\%$ for TJ3 ($n = 10$; $R = 1.9\ \Omega$), showing the formation of pinholes in the barrier.

We then normalized our $R(T)$ data according to $\frac{R(T)-R_{300\ \mathrm{K}}}{|R_{20\ \mathrm{K}}-R_{300\ \mathrm{K}}|}$. Figure 2(b) displays selected curves for different stages of barrier degradation (sample TJ2), obtained after performing the corresponding nth CIS cycle. Although the shapes of the (tunnel dominated) curves are almost equal, some display increasing R steps. On the other hand, the normalized metallic-dominated transport curves ($n > 6$) are all identical.

4. Discussion

We showed that local atomic displacements cause irreversible decreases in resistance and a progressive change of the dominant transport mechanism from tunnel to metallic, due to the interplay of two main contributions: tunnel transport through the undamaged part of the barrier (with resistance R_{t}) and metallic transport through pinholes (resistance R_{m}). We then write for the measured resistance (R):

$$\frac{1}{R} = \frac{1}{R_{\mathrm{t}}} + \frac{1}{R_{\mathrm{m}}}. \tag{4}$$

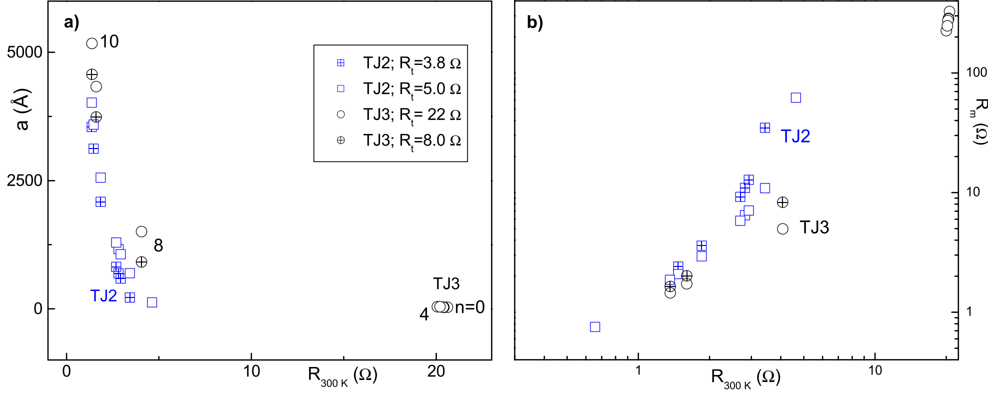

Figure 3. (a) Pinhole radius a, calculated using equation (8), as a function of the experimental TJ electrical resistance (TJ2 using $R_t = 3.8\ \Omega$ (open squares) and $R_t = 5\ \Omega$ (squares with crosses) and TJ3 using $R_t = 22\ \Omega$ (open circles) and $R_t = 8\ \Omega$ (circles with crosses; see discussion for details). (b) Corresponding metallic resistance R_m, as calculated from equation (4).

We can estimate the evolution of pinhole size with decreasing TJ resistance due to barrier degradation. The Sharvin theory predicts the resistance of a nanoconstriction modelled as a circular aperture of radius a (between two metallic layers) of electrical resistivity ρ and electron mean free path ℓ [23]. We then have in the ballistic limit ($\ell \gg a$):

$$R_m(\text{Sharvin}) = \frac{4\rho\ell}{3\pi a^2}. \tag{5}$$

Since the amorphous Ta layers of the studied TJs have a high resistivity ($\rho \approx 150\ \mu\Omega$ cm) [15], we do not expect the electron mean free path ℓ within a pinhole to be very large ($\ell \lesssim a$). We thus write the electrical resistance of a constriction in the diffusive regime ($\ell \ll a$), known as the Maxwell resistance [24]:

$$R_m(\text{Maxwell}) = \frac{\rho}{2a}. \tag{6}$$

A good approximation for the actual pinhole resistance (R_m) of a sample with finite ℓ is simply [24–26]:

$$R_m = R_m(\text{Maxwell}) + R_m(\text{Sharvin}). \tag{7}$$

To calculate the pinhole radius, let us assume that: (i) a pinhole is formed just after an irreversible resistance decrease under high applied current pulses; (ii) only one pinhole is formed and grows in the tunnel junction; and (iii) the tunnel resistance remains constant throughout the successive stages of degradation of CIS (significant R variation only arises from the enhancement of the metallic contribution). Accordingly, R_t is simply the TJ resistance measured before atomic displacement-induced barrier degradation ($R_t \approx 11\ \Omega$ for TJ2 and $R_t \approx 22\ \Omega$ for TJ3). This allows us to estimate the metallic resistance R_m using equation (4) and the measured R value (see figure 3(b)). Using equations (5)–(7), we can then express the pinhole radius as a function of ρ, ℓ and R_m:

$$a = \frac{3\pi\rho + \sqrt{3\pi\rho}\sqrt{64\ell R_m + 3\pi\rho}}{12\pi R_m}. \tag{8}$$

Using $\rho \approx 150\ \mu\Omega$ cm for the Ta layers (and pinholes) and assuming $\ell \approx 5$ Å, we can then estimate the pinhole radius (figure 3(a)). Notice that the actual pinhole composition is not entirely known, and the possibility of Ta–Al bonding cannot be excluded. However, the

migration of the Ta ions into the amorphous Al_2O_3 barrier should give rise to a disordered pinhole structure with a high resistivity. For TJ3, as expected, one obtains a pinhole radius which increases with decreasing resistance: from about 30 Å for $n = 4$ ($R_m = 250\ \Omega$) to 1500 Å for $n = 8$ ($R_m = 5\ \Omega$), and finally to 4300 Å for $n = 10$ ($R_m = 1.7\ \Omega$). Notice, however, that this simple model does not fully describe our data. In particular, it underestimates the metallic resistance: for $n = 8$ (for which we still observe tunnel-dominated transport; $\alpha < 0$) we obtain $R_m \approx 5\ \Omega$, which is already smaller than the (assumed constant) tunnel resistance, $R_t \approx 22\ \Omega$. Our model then predicts a metallic $R(T)$ behaviour for $n = 8$, which contradicts our data. Notice that such an R_m value depends only on R_t used in equation (4) and not on ρ or ℓ, which are used only to estimate a.

We conclude that the initial atomic displacement-driven irreversible resistance decrease is not due to the formation of pinholes (assumption (i)) but to the progressive weakening of the tunnel barrier (decreasing barrier thickness) and that the minimum experimental R value without pinholes ($R = R_t$) is considerably lower than the initial TJ resistance of 22 Ω. Using equation (4), we estimate that to ensure $R_t > R_m$ up to $n = 8$ we must have $R_t \approx 8\ \Omega$. Then, the initial 22 Ω → 8 Ω decrease in R corresponds only to a reduction in barrier thickness (δt) without the formation of pinholes. We estimate $\delta t \approx 1.3$ Å [15].

Assuming then that $R_t \approx 8\ \Omega$, we can calculate the new pinhole radius using equation (8) (figure 3(a)). For $n = 10$ we obtain $a = 900$ Å ($R_m = 8.3\ \Omega$) and for $n = 12$, $a = 3700$ Å ($R_m = 2.0\ \Omega$), which, nevertheless, are close to the values obtained above (considering $R_t \approx 22\ \Omega$). Furthermore, $R_t \approx 8\ \Omega$ is not the only value that adequately adapts to the observed $\alpha(R)$ dependence and we estimate $3.5\ \Omega \lesssim R_t \lesssim 8\ \Omega$. For $R_t \approx 3.5\ \Omega$ one has pinhole formation only for $n = 11$, already having $R_m < R_t$ ($a = 2500$ Å). In this case ($R_t \approx 3.5\ \Omega$), the formation of a pinhole immediately leads to metallic-dominated transport.

For TJ2, we have more α-values near the tunnel/metallic progressive transition, allowing us to estimate R_t within a narrower interval. First, notice that (as in the case of TJ3) if we use the initial TJ2 resistance ($R_t = R \approx 11\ \Omega$) to calculate R_m, we again obtain $R_m < R_t$ for a $R(T)$ data still dominated by tunnelling ($\alpha < 0$). Thus, we again conclude that there is initial progressive weakening of the tunnel barrier (decreasing barrier thickness), leading to a decrease of the TJ electrical resistance without formation of pinholes. We predict (using equation (4)) that $3.8\ \Omega \lesssim R_t \lesssim 5\ \Omega$ (figure 3), which corresponds to a decrease in barrier thickness satisfying $1.1\ \text{Å} \lesssim |\delta t| \lesssim 1.3$ Å. Using the two mentioned limiting R_t-values, we again observe that R_m decreases with decreasing TJ electrical resistance (figure 3(b)), denoting the increase in pinhole radius (figure 3(a)). In the case of TJ2, we observe that pinholes are already formed ($a \approx 1000$ Å) while $\alpha < 0$ (demonstrating tunnel-dominated transport; $R_m > R_t$). Further current-induced decrease of the TJ resistance is seen to be due to increase in the pinhole size, which enhances the metallic conductance and ultimately leads to metallic-dominated transport ($\alpha > 0$).

5. Conclusions

We showed that the initial degradation of the insulating barrier under high electrical currents arises from an irreversible decrease in barrier thickness ($\delta t \approx -1.3$ Å) due to localized displacement of ions from the electrodes into the barrier, without the formation of pinholes. Such barrier weakening leads to higher α values in our $R_b(T)$ and $R_B(T)$ measurements (with $\alpha_b > \alpha_B$), suggesting that irreversible and reversible switching arise from the same physical mechanism. Under adequate experimental conditions we might even reversibly switch between $\alpha_B < 0$ (tunnel-dominated transport) and $\alpha_b > 0$ (metallic-dominated transport), and vice

versa, by local current-driven ion diffusion. Such a phenomenon was recently observed by Deac *et al* [14] in ultra-thin TJs (barrier thickness $t = 5$ Å).

Increased barrier degradation leads to the formation of metallic paths between the two electrodes that, however, *do not lead to a metallic-dominated TJ transport* for small enough pinhole radius. The increase in pinhole radius gradually leads to the decrease of the metallic (Sharvin + Maxwell) resistance and thus to the ultimate dominance of metallic over tunnel transport.

Acknowledgments

This work ws supported in part by FEDER-POCTI/0155, POCTI/CTM/45252/02 and POCTI/CTM/59318/2004 from FCT and IST-2001-37334 NEXT MRAM projects. J Ventura is grateful for a FCT post-doctoral grant (SFRH/BPD/21634/2005).

References

[1] Moodera J S, Kinder L R, Wong T M and Meservey R 1995 Large magnetoresistance at room temperature in ferromagnetic thin film tunnel junctions *Phys. Rev. Lett.* **74** 3273–6

[2] Meservey R and Tedrow P M 1994 Spin-polarized electron tunneling *Phys. Rep.* **238** 173–243

[3] Wang D, Nordman C, Daughton J M, Zhenghong Q and Fink J 2004 70% TMR at room temperature for SDT sandwich junctions with CoFeB as free and reference layers *IEEE Trans. Magn.* **40** 2269–71

[4] Parkin S S P, Kaiser C, Panchula A, Rice P M, Hughes B, Samant M and Yang S H 2004 Giant tunnelling magnetoresistance at room temperature with MgO(100) tunnel barriers *Nat. Mater.* **3** 862–7

[5] Yuasa S, Nagahama T, Fukushima A, Suzuki Y and Ando K 2004 Giant room-temperature magnetoresistance in single-crystal Fe/MgO/Fe magnetic tunnel junctions *Nat. Mater.* **3** 868–71

[6] Yuasa S, Fukushima A, Kubota H, Suzuki Y and Ando K 2006 Giant tunneling magnetoresistance up to 410% at room temperature in fully epitaxial Co/MgO/Co magnetic tunnel junctions with bcc Co(001) electrodes *Appl. Phys. Lett.* **89** 042505

[7] Tehrani S, Engel B, Slaughter J M, Chen E, DeHerrera M, Durlam M, Naji P, Whig R, Janesky J and Calder J 2000 Recent developments in magnetic tunnel junction MRAM *IEEE Trans. Magn.* **36** 2752–7

[8] Slonczewski J C 1996 Current-driven excitation of magnetic multilayers *J. Magn. Magn. Mater.* **159** L1–7

[9] Berger L 1996 Emission of spin waves by a magnetic multilayer traversed by a current *Phys. Rev.* B **54** 9353–8

[10] Huai Y, Albert F, Nguyen P, Pakala M and Valet T 2004 Observation of spin-transfer switching in deep submicron-sized and low-resistance magnetic tunnel junctions *Appl. Phys. Lett.* **84** 3118–20

[11] Fuchs G D, Emley N C, Krivorotov I N, Braganca P M, Ryan E M, Kiselev S I, Sankey J C, Ralph D C, Buhrman R A and Katine J A 2004 Spin-transfer effects in nanoscale magnetic tunnel junctions *Appl. Phys. Lett.* **85** 1205–7

[12] Liu Y, Zhang Z, Freitas P P and Martins J L 2003 Current-induced magnetization switching in magnetic tunnel junctions *Appl. Phys. Lett.* **82** 2871–3

[13] Liu Y, Zhang Z and Freitas P P 2003 Hot-spot mediated current-induced resistance change in magnetic tunnel junctions *IEEE Trans. Magn.* **39** 2833–5

[14] Deac A, Redon O, Sousa R C, Dieny B, Nozières J P, Zhang Z, Liu Y and Freitas P P 2004 Current driven resistance changes in low resistance × area magnetic tunnel junctions with ultra-thin Al–O_x barriers *J. Appl. Phys.* **95** 6792–4

[15] Ventura J, Sousa J B, Liu Y, Zhang Z and Freitas P P 2005 Electromigration in thin tunnel junctions with ferromagnetic/nonmagnetic electrodes: nanoconstrictions, local heating, and direct and wind forces *Phys. Rev.* B **72** 094432

[16] Ventura J, Araujo J, Sousa J B, Liu Y, Zhang Z and Freitas P P 2006 Nanoscopic processes of current induced switching in thin tunnel junctions *IEEE Trans. Nanotechnol.* **5** 142–8

[17] Ventura J, Araujo J, Carpinteiro F, Sousa J B, Liu Y, Zhang Z and Freitas P P 2005 Relaxation phenomena in current induced switching in thin magnetic tunnel junctions *J. Magn. Magn. Mater.* **290** 1067–70

[18] Ventura J O, Sousa J B, Salgueiro da Silva M A, Freitas P P and Veloso A 2003 Anomalous magnetoresistance behavior of CoFe nano-oxide spin valves at low temperatures *J. Appl. Phys.* **93** 7690–2

[19] Ventura J, Araujo J P, Sousa J B, Ferreira R and Freitas P P 2007 Competing spin-dependent conductance channels in under-oxidized tunnel junctions *Appl. Phys. Lett.* **90** 032501

[20] Sorbello R S 1998 Theory of electromigration *Solid State Physics* vol 51, ed H Ehrenreich and F Spaepen (New York: Springer) pp 159–231
[21] Shang C H, Nowak J, Jansen R and Moodera J S 1998 Temperature dependence of magnetoresistance and surface magnetization in ferromagnetic tunnel junctions *Phys. Rev.* B **58** R2917–20
[22] Dimopoulos T, Gieres G, Wecker J, Luo Y and Samwer K 2004 Analysis of the magnetotransport channels in tunnel junctions with amorphous CoFeB *Europhys. Lett.* **68** 707–12
[23] Sharvin Y V 1965 A possible method for studying Fermi surfaces *J. Exp. Theor. Phys.* **48** 984–5
[24] Wexler G 1966 The size effect and the non-local Boltzmann transport equation in orifice and disk geometry *Proc. Phys. Soc.* **89** 927–41
[25] Ralls K S and Buhrman R A 1991 Microscopic study of $1/f$ noise in metal nanobridges *Phys. Rev.* B **44** 5800–17
[26] Nikolic B and Allen P B 1999 Electron transport through a circular constriction *Phys. Rev.* B **60** 3963–9